Biomech Model Mechanobiol (2009) 8:1–8
DOI 10.1007/s10237-007-0112-z

ORIGINAL PAPER

Estimating material parameters of human skin in vivo

Y. A. Kvistedal · P. M. F. Nielsen

Received: 18 July 2006 / Accepted: 6 November 2007 / Published online: 27 November 2007

Abstract An accurate mathematical representation of the mechanical behaviour of human skin is essential when simulating deformations occurring in the skin during body movements or clinical procedures. In this study constitutive stress–strain relationships based on experimental data from human skin in vivo were obtained. A series of multiaxial loading experiments were performed on the forearms of four age- and gender matched subjects. The tissue geometry, together with recorded displacements and boundary forces, were combined in an analysis using finite element modelling. A non-linear optimization technique was developed to estimate values for the material parameters of a previously published constitutive law, describing the stress–strain relationship as a non-linear anisotropic membrane. Ten sets of material parameters where estimated from the experiments, showing considerable differences in mechanical behaviour both between individual subjects as well as mirrored body locations on a single subject. The accuracy of applications that simulate large deformations of human skin could be improved by using the parameters found from the in vivo experiments as described in this study.

Y. A. Kvistedal (✉)
Norwegian Geotechnical Institute,
Sognsveien 72,
0855 Oslo, Norway
e-mail: kvistedal@gmail.com

Y. A. Kvistedal · P. M. F. Nielsen
Bioengineering Institute, University of Auckland,
70 Symond St, Auckland, New Zealand

1 Introduction

A detailed and accurate mathematical representation of the mechanical properties of human skin is important when using modelling to simulate the mechanical behaviour of the human body. As the skin is a continuous membrane covering almost the entire body, it has a major contribution to the total mechanical properties of various body parts, and should be included in corresponding numerical models. The mechanical behaviour of skin as an isolated organ is also important with respect to surgical techniques, as an accurate constitutive model could be used to simulate deformations relating to different types of incision and closing techniques. Many different experimental techniques have been proposed to measure the mechanical properties of skin. Some of the most common include suction tests (Alexander and Cook 1977; Elsner et al. 1990; Diridollou et al. 1998; Hendriks et al. 2003), torsion tests (Escoffier et al. 1989), indentation tests (Highley 1977), uniaxial tests (Snyder and Lee 1975), biaxial tests (Lanir and Fung 1974a; Schneider et al. 1984) and multiaxial tests (Reihsner et al. 1995). Recent work has tended to focus toward applying suction devices in combination with either an ultrasound (Diridollou et al. 2000, 2001; Hendriks et al. 2003; Dahan et al. 2004) or an OCT imaging device (Hendriks et al. 2004) to measure the stress distribution in deformed skin. These devices are, however, inadequate for modelling purposes as they do not account for the anisotropic nature of skin. Another trend has been to express the stress–strain relationship in terms of the Young's modulus (Escoffier et al. 1989; Diridollou et al. 2000, 2001). This too constitutes an oversimplification, ignoring the non-linear properties. Only a few attempts have successfully been made to experimentally determine the non-linear and anisotropic constitutive stress–strain properties of skin. These have been based on either biaxial or multiaxial in vitro experiments on

human (Reihsner et al. 1995) or animal specimens (Lanir and Fung 1974a). As the skin is believed to change its characteristics between the in vivo and in vitro states, the current study was designed to investigate human skin in vivo using a multiaxial approach. The obtained experimental data were used to estimate material parameters of a corresponding strain energy function on skin mechanics. The presented results are intended to improve applications where the nonlinear and anisotropic properties of human skin are simulated using large deformations.

Langer was the first to investigate residual tension and anisotropic behaviour in human skin (Langer 1861). From the observation that stab wounds from a circular object had ellipse shaped openings, he deduced that the amount of residual tension was dependent on direction. In his papers he sketched a set of lines for the entire body indicating the directions of maximum residual tension. Langer's lines are a phenomenological map of the anisotropy of human skin, and define a coordinate system for a constitutive model incorporating the anisotropic stress–strain properties. In clinical applications Langer's lines are commonly identified from folding lines, a technique also utilized in this study. Skin is in general anisotropic, non-linear, and exhibits viscoelastic behaviour (Payne 1991). The requirement for preconditioning, in order to achieve a repeatable stress–strain relationship between loading cycles, and loss of strain energy between loading and unloading cycles has been reported (Lanir and Fung 1974b). A common practice in mechanical experiments on soft tissue has been to use simplified quasistatic models to describe the observed behaviour. Using this approach tissue is commonly preconditioned by several loading cycles, with sufficient time between imposing deformations and acquiring force measurements to allow for stress relaxation to occur, before recording the deformations and applied loads. To complicate matters, differences in mechanical behaviour of skin have also been shown to be dependent on age, gender, body location, humidity, temperature and sun exposure (Alexander and Cook 1977; Schneider et al. 1984; Reihsner et al. 1995). In the current study the experiments were performed at identical body locations on a set of age- and gender matched human subjects, and in a controlled laboratory environment. This was done to investigate whether skin from comparable subjects would exhibit identical mechanical response upon the removal of most of these dependencies. Deriving a mathematical stress–strain relationship incorporating all the different components of soft tissue mechanics is difficult, and constitutive equations proposed for skin all involve some degree of simplification (Danielson 1973; Tong and Fung 1976; Lanir 1983; Bischoff et al. 2000). Tong and Fung derived a constitutive model describing the stress–strain behaviour of skin on a purely phenomenological basis, as an anisotropic and non-linear membrane using a quasistatic exponential strain energy function (Tong and Fung 1976).

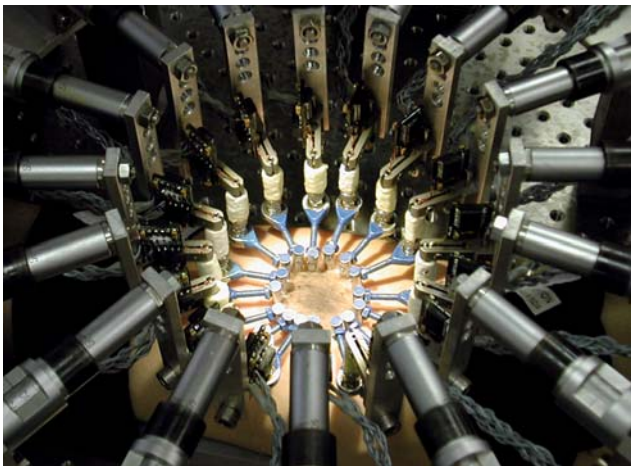

Fig. 1 The multiaxial testing rig with a subject's skin attached

A simplified form of this equation was used in the current study, and values for the material parameters obtained from multiple experiments.

2 Methods and materials

A previously described custom build multiaxial testing rig (Nielsen et al. 2002), Fig. 1, was used to investigate the stress-strain properties of human skin. The rig was equipped with sixteen *Physik Instrumente* DC-Mike M-226 actuators, capable of incremental motions of 0.2 µm over a range of of 50 mm. These were arranged as a circular array, allowing deformation to be imposed along eight separate axes. Each actuator was equipped with a custom-built 2D force transducer, from which the applied force vectors at each of the sixteen attachment points were recorded. The transducers had an operational range of ± 3 N and a SNR of 0.07%. An *Atmel* Camelia 4M CCD camera with 2048 $\times$ 2048 pixels was used to record the geometry and the internal deformations of the samples. The deformations of regions within the geometry were traced mathematically as displacements of 64 $\times$ 64 pixel subimages using a phase corrected crosscorrelation technique (Charette et al. 1997a,b; Malcolm et al. 2002). This technique could resolve displacements as small as 0.05 of a pixel, giving a resolution for the measured displacements of 1 µm.

The skin was mounted to the force transducers using an arrangement based on a miniature rod end bearing, as illustrated in Fig. 2. Due to the in vivo nature of the experiments it was not possible to obtain a perfectly flat skin sample. As a result of the connection to the subcutaneous tissue, the curvature in the skin surface also changed between the deformed states within the experiments. A fixed attachment to the actuators would have created unwanted vertical and torsional stresses in the sample and resulted in force measurement errors. By allowing the attachment points to move

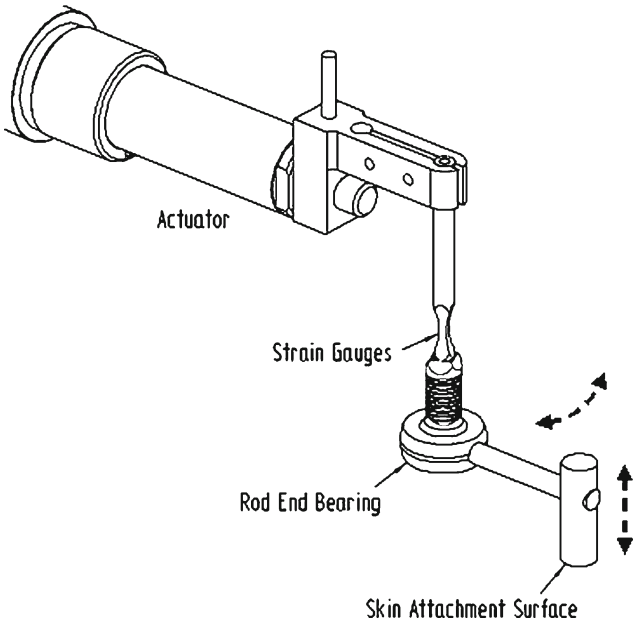

Fig. 2 Attachment mechanism used to mount the skin to the force transducers. The *dotted arrows* indicate the directions which allowed low friction movements

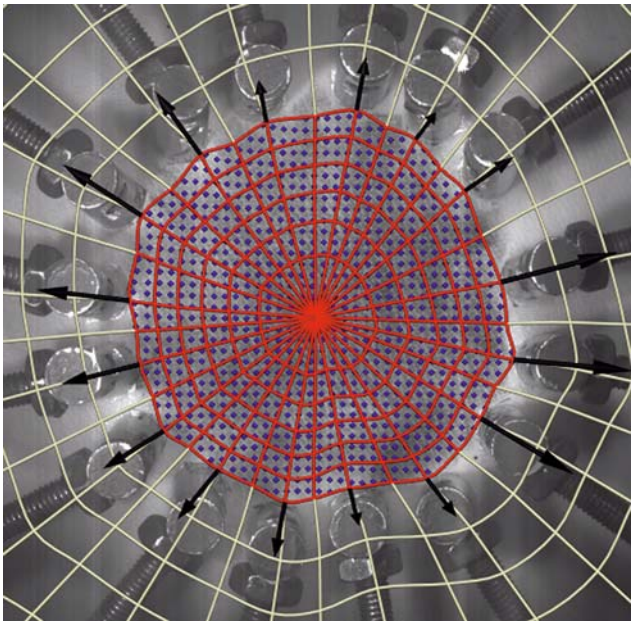

Fig. 3 The finite element model of in vivo human skin under multiaxial loading. Deformations of the sample (*red internal mesh*) are a result of the combined loading of applied forces (*black arrows*) and natural tension in the surrounding tissue (*white external mesh*). The constitutive stress–strain relationship was fitted to the measured displacements of a large set of internal data points (*blue points*)

freely in all directions except that of the applied force, the rod end bearings removed these constraints from the sample and cancelled any undefined forces from the measurements.

Appropriate ethics approval was obtained for the study and the participants were asked to supply written informed consent. The subjects were Caucasian males between 29 to 35 years of age, and all experiments were performed on the skin on the inner part of their forearm. Each subject's arm was mounted onto the multiaxial testing rig in a manner that allowed the subjects to maintain a relaxed position throughout the experiment. Two belts, one on each side of the test area, were used to restrain the arm. To obtain a rigid attachment, the skin within the test area was shaved and fine grained sandpaper used to remove dead cells from the skin's surface. The tip of the rod end bearings was attached to the surface of the skin using standard double sided tape. Finally, the skin was marked with a random distribution of fine grain carbon powder. This provided the high spatial resolution high contrast information required by the cross-correlation technique.

The samples used in the experiments were approximately 40 mm in diameter. From a reference state without any experimentally applied loads, an initial displacement of -1.0 mm was performed with all sixteen actuators, removing most of the residual tension from the sample. From this new compressed state a series of three incremental loading and unloading cycles were performed. The deformations were imposed by uniformly stretching the sample with increments of 0.2 mm on all sixteen actuators. After a 30 s interval, allowing the majority of stress relaxation to occur, the sample geometry and the boundary forces were recorded. The increments in deformation were repeated until the applied force measured by a majority of the force transducers exceeded 500 mN. In practice this was both subject- and loading cycle dependent, requiring between eleven and fifteen increments. The most highly deformed state of the samples was thus a 2.4–4.0 mm stretch from the reference state, along all eight axes. Once this criterion was met, releases of -0.2 mm were applied, and data recorded as above, until the starting point was reached. To obtain the best possible measurements the subject was asked to stay as motionless as possible for complete loading/unloading cycles. To ease discomfort short pauses were made between the three cycles, allowing the subject to obtain a more comfortable position. All deformations and force vectors were recorded relative to the reference state within each loading and unloading cycle. This ensured that distortions in or between cycles, caused by small movements made by the subject, would not affect the remaining measurements within the same experiment.

As there is no analytical solution for a soft tissue membrane deformed using a circular multiaxial rig, a finite element technique was used to analyse the skin experiments. Inhomogeneities in the strain field surrounding the attachment points have previously been reported in biaxial experiments on soft biological tissues (Nielsen et al. 1991). This further indicates the need for a mathematical representation of the geometry in order to obtain an accurate analysis of experimental data. The skin, as shown in Fig. 3, was modelled

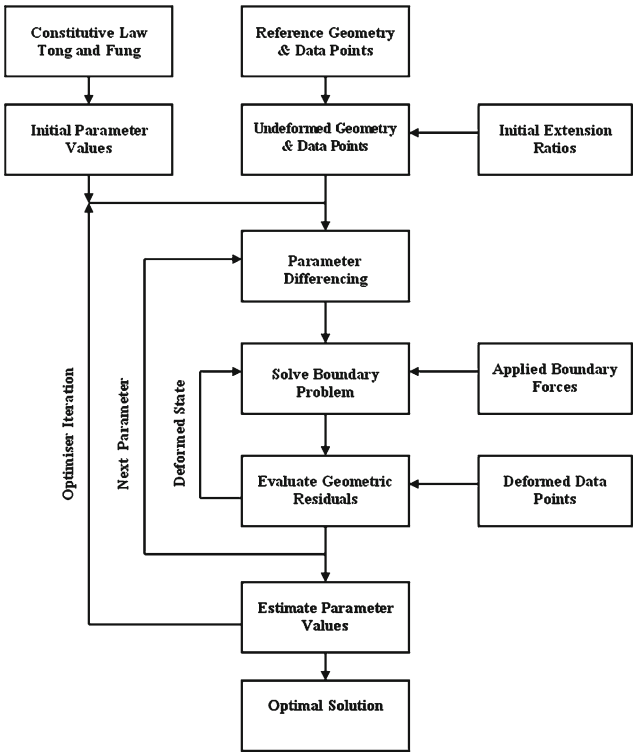

Fig. 4 Flow diagram of the parameter estimation algorithm used to determine the constitutive stress–strain relationship in in vivo human skin

in 2D using bi-cubic Hermite basis functions for the geometry. An internal circular mesh consisting of 192 elements represented the geometry of the sample. This was coupled to an external mesh, used to simulate the effects of the surrounding tissue. Specifying the axis of anisotropy thought the centre node was made possible using bi-linear Lagrange basis functions for the Langer lines and finite element software supporting multiple versions of these lines for each of the centre elements. The Langer lines were coupled to the geometry and allowed to deform with the sample. A grid of approximately 800 data points was placed inside the internal mesh, and the displacement of these traced between the deformed states.

In order to estimate values of the material parameters associated with the strain energy function, a forward solve algorithm (Augenstein et al. 2005) was developed, shown in Fig. 4, modelling skin as an incompressible membrane. A complication inherent in in vivo experiments is that skin is already prestretched in its reference state, due to coupling to the surrounding tissue. In order to account for the residual tension, initial extension ratios between the reference state and a stress free state were determined both along and across the Langer lines. This was achieved with a uniaxial compression system (Alexander and Cook 1977). Using this system the sample was compressed until wrinkling could be observed in the tissue surrounding the attachments. The tissue was then subsequently released to the point where the wrinkling disappeared, and the relative compression measured as the difference in distance between to central points initially 10 mm apart. The initial extension ratios were used to estimate a finite element geometry of the sample with the residual tension removed. This new stress free geometry was used as the undeformed geometry for the parameter estimation. During a forward solve two sets of boundary conditions were applied. The positions of the boundary nodes of the external mesh were fixed to the coordinates corresponding to the reference state. This, in effect, stretched the undeformed geometry back to the reference geometry, simulating the residual tension. The recorded force vectors were applied to the corresponding boundary nodes of the internal mesh, simulating the experimental loads. Starting with an initial estimate, the algorithm would loop through the parameters applying small increments to their value. After solving for each deformed state, geometric residuals were calculated from the difference between the predicted and measured displacements of the internal data points. Based on a least square fit to these residuals a non-linear optimization algorithm was used to refine the estimates for the parameters. The procedure was repeated between 2 and 5 times, depending on the experiment, until a specified tolerance level for convergence had been reached and an optimal solution for the material parameters found. Using this technique it was possible to obtain constitutive relationships for the stress–strain behaviour that incorporated the residual tension of skin in vivo, making it possible to use the current model to simulate both extension and compression.

The original version of the strain energy function used in this study (Tong and Fung 1976) has a total of thirteen material parameters, and is expressed as:

$$W = \frac{1}{2}\left(\alpha_1 e_1^2 + \alpha_2 e_2^2 + \alpha_3 e_{12}^2 + 2\alpha_4 e_1 e_2\right) + \frac{1}{2} c \exp\left(a_1 e_1^2 + a_2 e_2^2 + a_3 e_{12}^2 + 2a_4 e_1 e_2 + \gamma_1 e_1^3 + \gamma_2 e_2^3 + \gamma_4 e_1^2 e_2 + \gamma_5 e_1 e_2^2\right)$$

where the W is the strain energy, e_1 the strain along the Langer line, e_2 the strain across the Langer line and e_{12} the shear strain. In order to reduce the number of material parameters that required estimation, the higher order exponential terms $\gamma_{1\text{-}5}$ were, like in the original publication, set to zero. Initial attempts were made to obtain values for the shear and cross energy terms. The cross energy terms, α_4 and a_4, were consistently found to be at least three orders of magnitude smaller than the directional terms. As this made it difficult to obtain reasonable and consistent estimates, these parameters were also set to zero. No consistent value could be obtained for the shear terms, implying that little shear information was available in the type of deformations used in the experiments.

Table 1 Estimated material parameter values for the first loading cycle of experiments on four subjects

	α_1	α_2	c	a_1	a_2	RMS (mm)	Extension ratio$_1$	Extension ratio$_2$
Subject 1	75.61	60.41	5.431E-08	64.72	85.94	0.15	1.33	1.18
Subject 2	58.45	74.38	5.763E-06	54.60	150.49	0.13	1.28	1.14
Subject 3	71.28	71.98	8.537E-06	38.77	88.52	0.18	1.33	1.13
Subject 4a	37.01	48.57	1.812E-06	37.02	69.16	0.10	1.33	1.17
Subject 4b	47.56	47.96	2.254E-10	43.39	59.96	0.32	1.33	1.17

The parameter values for subject 4a and 4b were based on experiments conducted on the right and left arm. The RMS values were calculated from a least square fit between the measured displacements of the data points and the model predictions for a deformed state not used in the parameter estimation

While the exponential term, a_3 was set to zero, it was found important from numerical reasons to include the linear term α_3 in the parameter estimation. The obtained parameter values were, however, believed to originate from experimental artefacts, and thus not presented, as they did not constitute a useful description of the shear properties of human skin. The simplified form of the strain energy function as used in this study can be expressed as:

$$W = \frac{1}{2}\left(\alpha_1 e_1^2 + \alpha_2 e_2^2\right) + \frac{1}{2}c\exp\left(a_1 e_1^2 + a_2 e_2^2\right)$$

where the five estimated parameters were $\alpha_1, \alpha_2, c, a_1$ and a_2. The stress–strain relations are found by partial differentiation, giving:

$$S_1 = \alpha_1 e_1 + c a_1 e_1 \exp\left(a_1 e_1^2 + a_2 e_2^2\right)$$

$$S_2 = \alpha_2 e_2 + c a_2 e_2 \exp\left(a_1 e_1^2 + a_2 e_2^2\right)$$

where S_1 is the stress along the Langer line and S_2 the stress across the Langer line. These stresses were expressed in terms of the second Piola Kirchoff stress tensor, and the strains Lagrangian large strains. The stress equilibrium equations for large deformation theory were solved using finite elements (Zienkiewicz and Taylor 2000). These finite element solutions provided a relationship between the stresses in the skin and the forces and geometric deformations applied by the multiaxial rig.

3 Results

The material parameter values obtained for the first loading cycle of five different experiments, on four different subjects, are listed in Table 1. The stress–strain curves generated from the strain energy function, using these values, are shown in Fig. 5. Differences between the subjects were observed. Variations between individuals have previously been reported as being dependent on body locations and age (Schneider et al. 1984; Reihsner et al. 1995). The current study shows that differences in the stress–strain relationship must also be

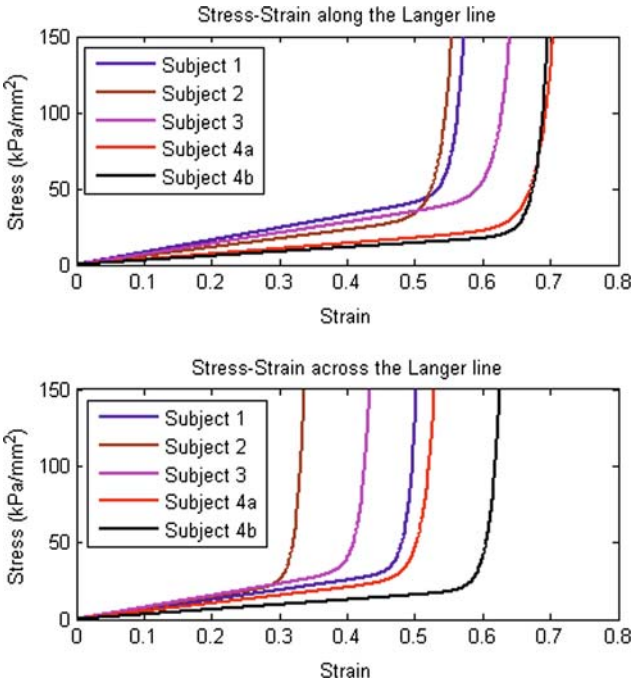

Fig. 5 Stress–strain curves generated from estimated parameter values for the first loading cycle of experiments on four different subjects

expected between age- and gender matched subjects at identical body locations.

The material parameters obtained from the three loading and unloading cycles of the experiment on subject 2 are shown in Table 2. The stress–strain curves generated from the strain energy function, using these values, are shown in Fig. 6. The similarities between the curves are an indication of the repeatability of both experimental and numerical processes used in this study. The difference between the curves furthermore illustrates the appropriateness of the constitutive model, as these are consistent with behaviour observed in many types of biological soft tissue. The effects of preconditioning between loading cycles, and the loss of strain energy between loading and unloading cycles, can be observed as changes in the slope between different sets of parameter values. The relative error between the measured deformations

Table 2 Estimated material parameter values from all three loading and unloading cycles of the experiment on subject 2

	α_1	α_2	c	a_1	a_2	RMS (mm)
Loading cycle 1	58.45	74.38	5.763E-06	54.60	150.49	0.13
Unloading cycle 1	46.68	97.82	1.096E-05	48.95	132.82	0.09
Loading cycle 2	69.78	80.83	1.148E-05	50.33	143.52	0.11
Unloading cycle 2	44.68	69.52	3.221E-05	46.68	120.02	0.22
Loading cycle 3	49.56	34.91	8.819E-05	42.06	123.02	0.13
Unloading cycle 3	49.19	76.52	8.125E-06	50.77	135.56	0.19

The RMS values were calculated from a least square fit between the measured displacements of the data points and the model predictions for a deformed state not used in the parameter estimation

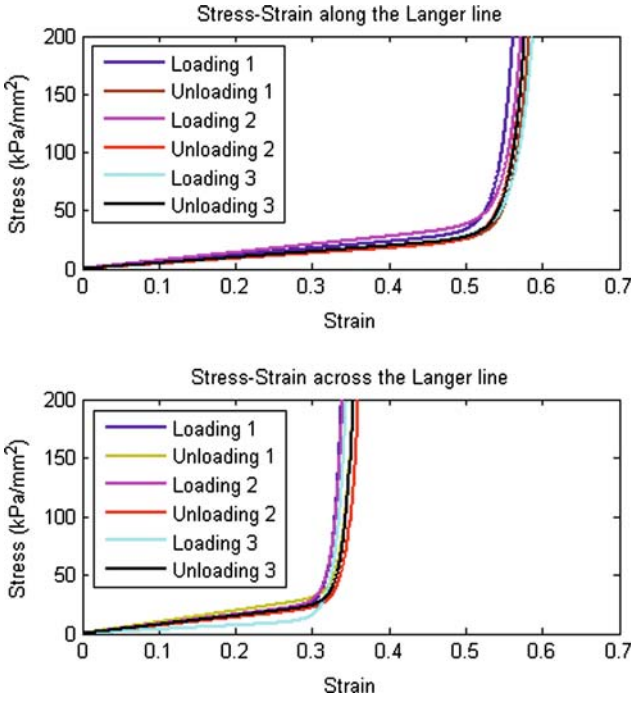

Fig. 6 Stress–strain curves generated from the estimated parameter values for all three loading and unloading cycles on a single subject

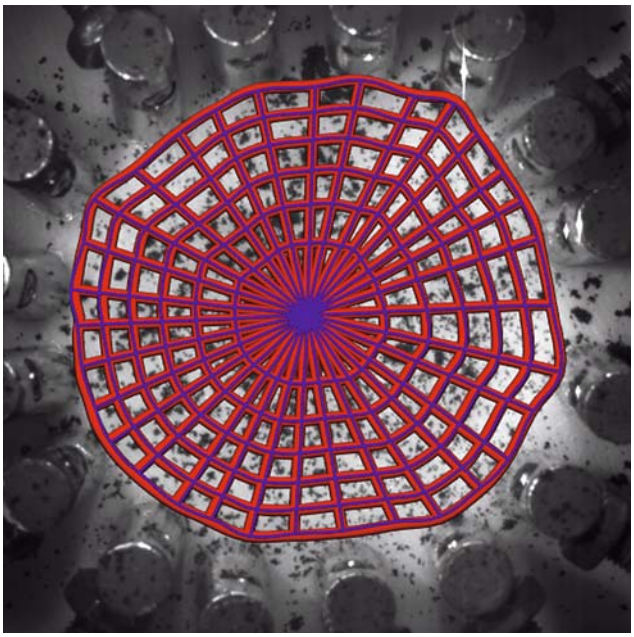

Fig. 7 Deformations as predicted by the model (*thin blue mesh*) superimposed on the measured deformations (*thick red mesh*) of a deformed state not used in the parameter estimation. RMS = 0.13 mm

and the model predictions for the first loading cycle of the experiment on subject 2 are illustrated in Fig. 7.

4 Discussion

There are several advantages in using circular multiaxial loading to investigate the stress–strain properties of soft tissue membranes. A biaxial experiment is limited in that it can only be applied to samples with a single structural direction and parallel fibres. As many types of biological soft tissue are found to have more complex or inhomogeneous fibre fields, it is often necessarily to use small samples in order to be able to interpret the data. To extract the stress–strain relationship for an anisotropic constitutive model, such as the one used in this study, the fibre direction also has to be aligned with the loading axes. Such limitations are not inherent to multiaxial experiments. When combined with appropriate modelling techniques, it has previously been shown that multiaxial loading tests can be used to investigate large inhomogeneous samples (Malcolm et al. 2002). Due to the complexity of the mechanical deformations imposed during multiaxial loading experiments, there is a lack of force–displacement data for the structural directions that can be interpreted directly. Numerical techniques, with mathematical representations of the tissues geometry and structure, are therefore required in order to extract the constitutive stress–strain relationship.

An inherent complication to mechanical testing of human skin in vivo is the coupling to the subcutaneous and surrounding tissue. Skin in vivo should ideally be modelled in 3D, incorporating the skin layers and the subcutaneous tissue. If

such a physiological model was used to analyse experimental data, detailed 3D information about the structure, together with a known constitutive representation of the subcutaneous tissue, would be required. As none of these were available, the coupled mechanical behaviour of the skin and the subcutaneous tissue, were in the current study estimated using a simplified 2D incompressible model. It is uncertain whether skin fully satisfies the criteria of incompressibility, but the numerical errors introduced by this simplification are in this context assumed to be minor. The residual tension in skin in vivo constitutes an important part of the total mechanical behaviour that needs to be incorporated into a constitutive model. No ideal method has, however, been found to quantify this effect at a single location. Future improvements could be made by developing new methods to replace the uniaxial compression technique used in this study.

The importance of obtaining data during the first loading cycles of mechanical experiments, in order to record the effects of preconditioning, is vital in order to obtain a full understanding of the stress–strain behaviour of soft biological tissues (Humphrey 1995). Recent studies on tissue from rat hearts have further questioned the practice of preconditioning, on the basis of tissue viability (Emery et al. 1997; Kirton et al. 2004). The effects of preconditioning are, in these studies, considered to be a result of damage inflicted by repeated deformations beyond the physiological range, or as a result of tissue degradation during in vitro experiments. In the current study the skin was subjected to large deformations beyond the range occurring during normal body movements, and the effects of preconditioning were observed. After the experiment it was noted that the skin was inflamed for about 1 h, indicating that damage had occurred within the tissue (Peacock et al. 1996). When simulating mechanical behaviour of human skin, it is important to consider the nature of the deformations and to choose data from similar experimental conditions. If it is important to recreate the behaviour of the first cycle of specific phenomena, then, by definition, data from preconditioned tissue will not be suitable as such a model will represent the behaviour after repeated deformation cycles.

The constitutive relationships obtained in this study are a detailed and accurate mathematical representation of the mechanical behaviour of the skin from the inner part of the forearm on a set of age- and gender matched subject. The observed differences extend previously reported results, demonstrating variations dependent on age, gender and body location. These findings imply that accurate predictions for an individual skin sample can only be obtained if the simulations are based on experimental data and estimated material parameter values from the same sample. Caution must therefore be applied when using the constitutive relationships presented in this study to simulate different types of mechanical skin problems, as the variations demonstrated between different types of human skin will introduce uncertainties to such predictions. However we contend that the mathematical model and generalized parameters described in this study allows computationally efficient and accurate simulations of skin under a range of deformations.

The mechanical properties of human skin are in general non-linear, anisotropic and strain rate dependent. In order to accurately simulate the behaviour of human skin for the most commonly occurring mechanical deformations, a constitutive equation would need to account for all of these dependencies. The results obtained in this study have shown that there are differences in the relative stiffness of skin from different individuals, and that these cannot be explained by gender, body location or environmental variables. Although it is difficult to make any conclusions with respect to the physiological basis for the observed differences from force versus displacement measurements, it is apparent that a constitutive equation needs to account for these differences. In the absence of a physiological based explanation, this is achieved by estimating different material parameter values for each sample. The experimental protocol used in this study was chosen to measure stress relaxed quasistatic deformations, in order to closely emulate specific clinical applications. As a result the applicability of the obtained results are limited to comparable situations, where one is studying static deformations and stresses that occur after an initial load has been applied. Developing new experimental apparatus and utilizing a strain rate dependent constitutive equation, could extend the described parameter estimation method to obtain a full viscoelastic description of the stress–strain relationship for in vivo human skin, and to further close the gap between mechanics and biology.

References

Alexander H, Cook TH (1977) Accounting for natural tension in the mechanical testing of human skin. J Investigative Dermatol 69(3):310–314

Augenstein KF, Cowan BR, LeGrice IJ, Nielsen PM, Young AA (2005) Method and apparatus for soft tissue material parameter estimation using tissue tagged magnetic resonance imaging. J Biomechanical Eng 127(1):148–157

Bischoff JE, Arruda EM, Grosh K (2000) Finite element modeling of human skin using an isotropic, nonlinear elastic constitutive model. J Biomechanics 33(6):645–652

Charette PG, Hunter IW, Hunter PJ (1997a) Large deformation mechanical testing of biological membranes using speckle interferometry in transmission. I: Experimental apparatus. Appl Opt 36(10):2238–2245

Charette PG, Hunter IW, Hunter PJ (1997b) Large deformation mechanical testing of biological membranes using speckle interferometry in transmission. II: Finite element modeling. Appl Opt 36(10):2246–2251

Dahan S, Lagarde JM, Turlier V, Courrech L, Mordon S (2004) Treatment of neck lines and forehead rhytids with a nonablative 1540-nm Er:Glass Laser: a controlled clinical study combined with

the measurement of the thickness and the mechanical properties of the skin. Dermatol Surgery 30(6):872–880

Danielson DA (1973) Human skin as an elastic membrane. J Biomechanics 6(5):539–546

Diridollou S, Berson M, Vabre V, Black D, Karlsson B, Auriol F, Gregoire JM, Yvon C, Vaillant L, Gall Y, Patat F (1998) An in vivo method for measuring the mechanical properties of the skin using ultrasound. Ultrasound Med Biol 24(2):215–224

Diridollou S, Black D, Lagarde JM, Gall Y, Berson M, Vabre V, Patat F, Vaillant L (2000) Sex- and site-dependent variations in the thickness and mechanical properties of human skin in vivo. Int J Cosmetic Sci 22(6):421–435

Diridollou S, Vabre V, Berson M, Vaillant L, Black D, Lagarde JM, Gregoire JM, Gall Y, Patat F (2001) Skin ageing: changes of physical properties of human skin in vivo. Int J Cosmetic Sci 23:353–362

Elsner P, Wilhelm D, Maibach HI (1990) Properties of human forearm and vulvar skin. Br J Dermatol 122(5):607–614

Emery JL, Omens JH, McCulloch AD (1997) Strain softening in rat left ventricular myocardium. J Biomechanical Eng 119(1):6–12

Escoffier C, de Rigal J, Rochefort A, Vasselet R, Leveque JL, Agache PG (1989) Age-related mechanical properties of human skin: an in vivo study. J Investigative Dermatol 93(3):353–357

Hendriks FM, Brokken D, van Eemeren JTWM, Oomens CWJ, Baaijens FPT, Horsten JBAM (2003) A numerical-experimental method to characterize the non-linear mechanical behaviour of human skin. Skin Res Technol 9(3):274–283

Hendriks FM, Brokken D, Oomens CWJ, Baaijens FPT (2004) Influence of hydration and experimental length scale on the mechanical response of human skin in vivo, using optical coherence tomography. Skin Res Technol 10(4):231–241

Highley KR (1977) Frictional properties of skin. J Investigative Dermatol 69(3):303–305

Humphrey JD (1995) Mechanics of the arterial wall: review and directions. Crit Rev Biomed Eng 23(1–2):1–162

Kirton RS, Taberner AJ, Young AA, Nielsen PM, Loiselle DS (2004) Strain softening is not present during axial extensions of rat intact right ventricular trabeculae in the presence or absence of 2,3-butanedione monoxime. Am J Physiol Heart Circulatory Physiol 286(2):H708–715

Langer K (1861) On the anatomy and physiology of the skin I-IV. Sitzungsbericht der Academie der Wissenschaften in Wien. Translated and reprinted: (1978). Br J Plastic Surgery 31:3–8, 93–106, 185–199, 273–278

Lanir Y (1983) Constitutive equations for fibrous connective tissues. J Biomechanics 16(1):1–12

Lanir Y, Fung YC (1974a) Two-dimensional mechanical properties of rabbit skin. I. Experimental system. J Biomechanics 7(1):29–34

Lanir Y, Fung YC (1974b) Two-dimensional mechanical properties of rabbit skin. II. Experimental results. J Biomechanics 7(2):171–182

Malcolm DT, Nielsen PM, Hunter PJ, Charette PG (2002) Strain measurement in biaxially loaded inhomogeneous, anisotropic elastic membranes. Biomechanics Model Mechanobiol 1(3):197–210

Nielsen PM, Hunter PJ, Smaill BH (1991) Biaxial testing of membrane biomaterials: testing equipment and procedures. J Biomechanical Eng 113(3):295–300

Nielsen PM, Malcolm DT, Hunter PJ, Charette PG (2002) Instrumentation and procedures for estimating the constitutive parameters of inhomogeneous elastic membranes. Biomechanics Model Mechanobiol 1(3):211–218

Payne PA (1991) Measurement of properties and function of skin. Clin Phys Physiol Meas 12(2):105–129

Peacock LJ, Lawrence WJ, Peacock EE (1996) Wound healing. The physiological basis of surgery. J. P. O'Leary and L. R. Capote. Williams & Wilkins, Louisiana

Reihsner R, Balogh B, Menzel EJ (1995) Two-dimensional elastic properties of human skin in terms of an incremental model at the in vivo configuration. Med Eng Phys 17(4):304–313

Schneider DC, Davidson TM, Nahum AM (1984) In vitro biaxial stress–strain response of human skin. Arch Otolaryngol 110(5):329–333

Snyder RW, Lee LH (1975) Experimental study of biological tissue subjected to pure shear. J Biomechanics 8(6):415–419

Tong P, Fung YC (1976) The stress–strain relationship for the skin. J Biomechanics 9(10):649–657

Zienkiewicz OC, Taylor RL (2000) The finite element method—solid mechanics. Butterworth-Heinemann, Oxford